

Thin nematic films: anchoring effects and stripe instability revisited

O V Manyuhina¹ and M Ben Amar²

¹ Nordita, Royal Institute of Technology & Stockholm University, Roslagstullsbacken 23, SE-10691 Stockholm, Sweden

² Laboratoire de Physique Statistique, Ecole Normale Supérieure, UPMC Univ Paris 06, Université Paris Diderot, CNRS, 24 rue Lhomond, 75005 Paris, France

Preprint NORDITA 2012-048

Abstract. We examine theoretically the role of anchoring effects in nematic films of submicron thickness spread on liquid substrates. The competing boundary conditions and the saddle-splay elasticity may cause the periodic undulations of the director, characterising the stripe state. We conjecture four different base states for the nematic director depending on the thickness of the film and the anchoring strengths: i) planar, ii) hybrid aligned nematic (HAN), iii) twisted and iv) twist-bended. The planar and HAN base states become linearly unstable with respect to the perturbation of the wavevector in the direction orthogonal to the initial state. However, the wavelength at the bifurcation is finite only in presence of nonzero azimuthal anchoring at either of the two interfaces. The presence of azimuthal anchoring at both interfaces results in the twisted base state and the possibility of periodic distortions in mutually orthogonal directions. Our theoretical findings give insight into recent experimental observations of cyanobiphenyl liquid crystals deposited on water and glycerol [A. M. Cazabat *et al.*, *Adv. Colloid Interface Sci.* **168**, 29 (2011)].

1 Introduction

Nematic liquid crystals (LC) sandwiched between two solid surfaces were extensively studied during the last five decades, resulting in numerous applications, e.g. liquid crystal display. About twenty years ago, the pioneering works by Lavrentovich, Sparavigna and Pergamenschchik [1,2,3,4] considered fascinating systems, namely the spontaneous spreading of 5CB (4-pentyl-4'-cyanobiphenyl LC) on liquid substrate such as glycerol. These authors observed the formation of spatially-periodic stripes resulting from the competition between the surface and volume energy namely between the boundary conditions and the elastic bulk anisotropy of nematic LC. The period L of the stripe domains is controlled by the thickness h of the film in a non-trivial way, yielding the ratio $L/h \propto 100$ for different LC systems [5]. The presence of the free nematic-air interface allows the thickness of the spreading film to be adopted by the film itself rather than being a fixed parameter. Recent experiments by the group of A. M. Cazabat [5,6,7,8,9] suggest that the stripe phase occurs within the range of thickness $h_{c1} \leq h \leq h_{c2}$, where the lower threshold $h_{c1} \simeq 20\text{--}30\text{ nm}$ and the upper threshold $h_{c2} \simeq 0.5\text{--}0.6\text{ }\mu\text{m}$ seem to be independent of the type of substrate and the LC molecules. The lower threshold, giving the instability from the uniform planar state towards the stripe state, was identified recently within an analytic framework [10]. The resulting critical thickness and the critical wavenumber were compared with experimental data, pointing out the essential role of the azimuthal anchoring. Finding the upper thresh-

old, which describes the instability from the hybrid aligned nematic (HAN) state towards the stripe state, requires the extension of the approach developed in [10,11,12] and is one of the subjects of the present paper.

The study of the stripe instability of nematic films spread on liquid substrates helps to identify the parameters entering the macroscopic free energy of interfaces. Still the role of these parameters remains a question of debate. One of the first models [1], considering perturbations of the HAN base state, suggests the crucial role of the splay-bend elastic constant K_{13} for obtaining the best fit of experimental data. The predictions of another model [4] indicates the dependence of the threshold thickness h_{c1} and h_{c2} on the saddle-splay elastic constant K_{24} , while the wavelength of stripes was not determined. More recent analysis [10] shows that without accounting for azimuthal anchoring, the wavelength of stripes at threshold is infinite, in contradiction with experimental observations [4,5,7,8,9]. The presence of azimuthal anchoring at one of the interfaces penalises strong in-plane distortions of the nematic director (stripe domains) and favours the common alignment of the molecules. However, the azimuthal anchoring is not an intrinsic parameter of the system, it is rather induced by the thickness gradient at the edge of the nematic film [4,13] or by magnetic fields [3,14], contrary to the polar anchoring which does not depend on a particular experiment and is known *a priori* [7,15]. According to [16] the value of the azimuthal anchoring should be one or two orders of magnitude smaller than the polar anchoring. By analysing the threshold for the formation

of stripes Sparavigna et al [3] estimated the extrapolation length for the azimuthal anchoring of 5CB at the air interface, such as $10 - 100 \mu\text{m}$, assuming infinitely strong planar anchoring at 5CB–glycerol interface.

Nevertheless, none of the proposed models indicates the possible formation of a long-wavelength square pattern for the submicron range of thickness, as observed in the recent experiments [5,7]. Plausibly, the reason for such theoretical limitation is related to the perturbation approach and the assumption of an idealised base state, such as planar or HAN nematic. These states are linearly unstable only with respect to the perturbation of the wavevector in the direction orthogonal to the initial state. In this paper we take into account a finite azimuthal anchoring at both interfaces, resulting in a small twist (or twist-bend) of the director along the thickness of the film. Hence, we show that the perturbation of the twisted state can account for stripe instability in mutually orthogonal directions, which can be compared with the experimental observations of squared structures.

The paper is organised as follows. First we reexamine the possible base state of thin films spread on liquid substrate, assuming the in-plane degeneracy of the boundary conditions. Then we perform the linear stability analysis to identify the lower and the upper instability thresholds towards the stripe phase, starting from the planar and the HAN base states. In section 5 we present the results of the linear stability analysis for the twisted state. We analyse the effects of saddle-splay constant K_{24} as well as azimuthal anchoring on the critical thickness, wavelength and the amplitude of stripes at the bifurcation point.

2 Formulation of the problem

Nematic liquid crystals are described by the unit vector \mathbf{n} , called the director, characterising the averaged orientation of molecules. The free energy associated with distortions of this director in space is given by

$$\mathcal{F}_{el} = \frac{1}{2} \int_V dV \left[K |\nabla \mathbf{n}|^2 - K_{24} \nabla \cdot (\mathbf{n} (\nabla \cdot \mathbf{n}) + \mathbf{n} \times \nabla \times \mathbf{n}) \right], \quad (1)$$

where we have assumed the one-constant approximation of the Oseen–Zocher–Frank free energy [17], quadratic in the director derivatives. The elastic constant K stands for the equal splay, twist and bend elastic moduli [18], while the saddle-splay elastic constant K_{24} should satisfy the Ericksen’s inequalities [19]

$$|K_{24}| \leq K, \quad K \geq 0, \quad (2)$$

which guarantee the stability of the uniform nematic state $\mathbf{n} = \text{const}$. The uniformly aligned director configuration can become unstable in presence of the competing boundary conditions and the saddle-splay elastic term, favouring the distorted configuration of the nematic director. Therefore the modulated stripe state can be achieved, when the saddle-splay contribution to the free energy becomes substantial, which is plausibly realised in *thin* nematic films with *weak* anchoring boundary conditions.

For convenience we parametrise the director as

$$\mathbf{n} = \sin \theta \cos \varphi \mathbf{e}_x + \sin \theta \sin \varphi \mathbf{e}_y + \cos \theta \mathbf{e}_z, \quad (3)$$

where θ and φ are the polar and the azimuthal angles, depending on the Cartesian coordinates x, y, z . The first term of the free energy (1) integrated over the volume V characterises the bulk contribution and within the parametrisation (3) can be rewritten as

$$\mathcal{F}_b = \frac{K}{2} \int_V dV (|\nabla \theta|^2 + \sin^2 \theta |\nabla \varphi|^2), \quad (4)$$

while the last divergence term can be transformed into the surface integral as

$$\mathcal{F}_s = -\frac{K_{24}}{2} \int_S dS \left[\cos \varphi (\partial_x \theta + \cos \theta \sin \theta \partial_y \varphi) + \sin \varphi (\partial_y \theta - \cos \theta \sin \theta \partial_x \varphi) \right] \Big|_{z=0}^{z=h}. \quad (5)$$

where h is the thickness of the nematic film and the surface normal is parallel to the z -axis.

Usually, liquid crystals are considered to be in contact with solid substrates, which favour the alignment of the director \mathbf{n} along their easy axis, characterised by the polar angle $\bar{\theta}$ and the azimuthal angle $\bar{\varphi}$. These anisotropic interactions between liquid crystal and surface on the macroscopic scale can be expressed by introducing an effective energy $W(\theta - \bar{\theta}, \varphi - \bar{\varphi})$ [20], depending on the orientation of the director at the interface with respect to the easy axis, which in general is written as a sum of spherical harmonics. Up to the lowest (symmetry allowed) order, we assume the following phenomenological expression for the interfacial energy, which should be added to the elastic free energy (1)

$$\mathcal{F}_a = \sum_{i=1,2} \int_S dS \left[\frac{W_{\theta_i}}{2} \sin^2(\theta_i - \bar{\theta}_i) + \frac{W_{\varphi_i}}{2} \sin^2 \theta_i \sin^2(\varphi_i - \bar{\varphi}_i) \right], \quad (6)$$

accounting for the polar and degenerate azimuthal anchoring (see sect. 3 for additional arguments) at two interfaces denoted by index i . Here W_{θ_i} and W_{φ_i} are the polar and the azimuthal anchoring strengths, which define the energy cost for the deviation of the director from the easy axis along the normal to the interface (z -axis) and parallel to the plane of the interface (xy -plane), accordingly. In the case of our interest the nematic–liquid substrate interface with $i = 1$ ($z = 0$) is characterised by the preferred orientation of the director $\bar{\theta}_1 = \pi/2$ (planar anchoring), and at the nematic–air interface with $i = 2$ ($z = h$) we have a homeotropic anchoring with $\bar{\theta}_2 = 0$. From the experimental works [4,7] we know that the planar anchoring W_{θ_1} is stronger than the homeotropic anchoring W_{θ_2} , and quantitatively the extrapolation lengths for 5CB on glycerol system are $L_{\theta_2} = K/W_{\theta_2} = 0.7 \mu\text{m}$ and $L_{\theta_1} = K/W_{\theta_1} = 0.35 \mu\text{m}$.

The azimuthal anchoring is not fixed *a priori* and we will consider two situations below i) the vanishing anchoring at the nematic–air interface $W_{\varphi_2} = 0$ and thus the

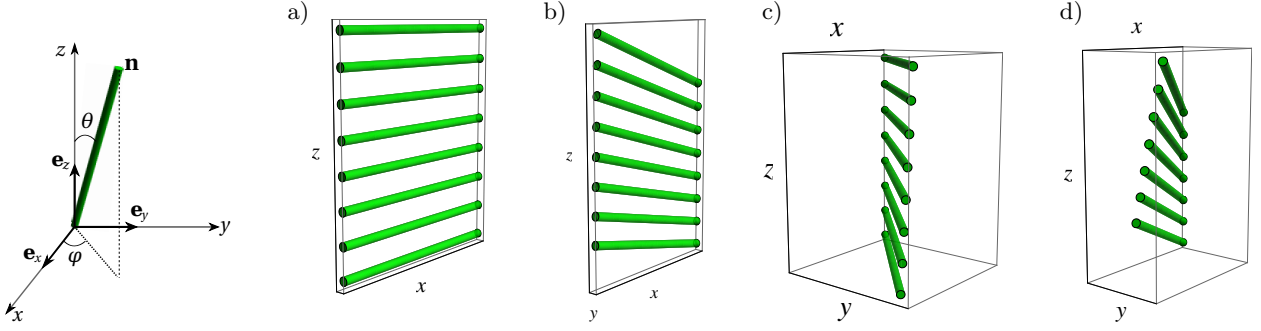


Fig. 1. An example of four base states, where the director \mathbf{n} (3) varies along the thickness of the film (z -axis) according to (9). The parameters are chosen as $L_{\theta_1} = 0.35 \mu\text{m}$, $L_{\theta_2} = 0.7 \mu\text{m}$ [7,15] a) $h = 0.1 \mu\text{m}$, $L_{\varphi_1} = 1 \mu\text{m}$ and $L_{\varphi_2} = 2 \mu\text{m}$ (planar), b) $h = 0.2 \mu\text{m}$, $L_{\varphi_1} = 1 \mu\text{m}$ and $L_{\varphi_2} = 2 \mu\text{m}$ with $\theta_2 - \theta_1 \approx 0.12$ (HAN), c) $h = 0.1 \mu\text{m}$, $L_{\varphi_1} = L_{\varphi_2} = 2 \mu\text{m}$ with $\varphi_2 - \varphi_1 \approx 0.05$ (twisted), d) $h = 0.3 \mu\text{m}$, $L_{\varphi_1} = L_{\varphi_2} = 2 \mu\text{m}$ with $\theta_2 - \theta_1 \approx 0.03$, and $\varphi_2 - \varphi_1 \approx 0.08$ (twist-bend).

base state is confined to the 2D plane with $\varphi = \bar{\varphi}_1$ ii) the non-zero azimuthal anchoring at both interfaces and if $\bar{\varphi}_2 \neq \bar{\varphi}_1$ the twist is accommodated in the base state. The actual angles $\theta_1 \equiv \theta(0)$, $\theta_2 \equiv \theta(h)$ and $\varphi_1 \equiv \varphi(0)$, $\varphi_2 \equiv \varphi(h)$ entering (6) should satisfy the boundary conditions, derived in the following section. All the results from now on will be written in terms of a dimensionless coordinate $\tilde{z} = z/h$.

3 Base state of nematic films

Firstly, we assume that the angles $\theta(\tilde{z})$ and $\varphi(\tilde{z})$ depend only on the coordinate $\tilde{z} = z/h$ along the thickness of the film. In this case the surface contribution (5) due to the saddle-splay elasticity (5) vanishes. The Euler-Lagrange equations associated with the bulk free energy (4) are

$$\partial_{\tilde{z}\tilde{z}}\theta - \sin\theta \cos\theta (\partial_{\tilde{z}}\varphi)^2 = 0, \quad (7a)$$

$$\partial_{\tilde{z}}(\sin^2\theta \partial_{\tilde{z}}\varphi) = 0. \quad (7b)$$

The first integral is

$$\partial_{\tilde{z}}\varphi = \frac{B_1}{\sin^2\theta}, \quad (\partial_{\tilde{z}}\theta)^2 = B_2^2 - \frac{B_1^2}{\sin^2\theta}, \quad (8)$$

and the second one yields the solutions θ and φ , written in the following form

$$\cos\theta(\tilde{z}) = \frac{\sin(B_3 - B_2\tilde{z})}{\sqrt{B_2^2/(B_2^2 - B_1^2)}}, \quad (9a)$$

$$\tan(\varphi(\tilde{z}) + B_4) = \frac{B_1}{B_2} \tan(B_2\tilde{z} - B_3). \quad (9b)$$

Let us consider several limiting cases:

- a) $\theta_1 = \theta_2 = \pi/2$ and $\varphi_1 = \varphi_2$, ($B_1 = 0$, $B_2 = 0$), **planar** state with uniformly aligned director \mathbf{n} ,
- b) $\theta(\tilde{z}) = \theta_1 + (\theta_2 - \theta_1)\tilde{z}$ and $\varphi_1 = \varphi_2$, ($B_1 = 0$), **HAN** state with θ varying along the thickness of the film

- c) $\theta_1 = \theta_2 = \pi/2$ and $\varphi(\tilde{z}) = \varphi_1 + (\varphi_2 - \varphi_1)\tilde{z}$, ($B_2^2 = B_1^2$), **twisted** state with φ varying along the thickness,

- d) $\theta_1 \neq \theta_2$ and $\varphi_1 \neq \varphi_2$, satisfying (9), (10), **twist-bend**.

In Fig. 1 we show an example of four base states, assuming the submicron thickness h of nematic film and the extrapolation lengths L_{θ_i} and L_{φ_i} .

In general, the integration constants B_i should be determined from the boundary conditions associated with (4) and (6) expressed as

$$2\partial_{\tilde{z}}\theta|_{\tilde{z}=0} + \sin 2\theta_1 \left(\frac{h}{L_{\theta_1}} - \frac{h}{L_{\varphi_1}} \sin^2 \varphi_1 \right) = 0, \quad (10a)$$

$$2\partial_{\tilde{z}}\theta|_{\tilde{z}=1} + \sin 2\theta_2 \left(\frac{h}{L_{\theta_2}} + \frac{h}{L_{\varphi_2}} \sin^2(\varphi_2 - \bar{\varphi}_2) \right) = 0, \quad (10b)$$

$$\sin^2 \theta_1 \left(2\partial_{\tilde{z}}\varphi|_{\tilde{z}=0} - \frac{h}{L_{\varphi_1}} \sin 2\varphi_1 \right) = 0, \quad (10c)$$

$$\sin^2 \theta_2 \left(2\partial_{\tilde{z}}\varphi|_{\tilde{z}=1} + \frac{h}{L_{\varphi_2}} \sin^2 \theta_2 \sin 2(\varphi_2 - \bar{\varphi}_2) \right) = 0, \quad (10d)$$

where L_{θ_i} and L_{φ_i} are the extrapolation lengths for polar and azimuthal anchoring, respectively, $L_{\theta_2} > L_{\theta_1}$ (the planar anchoring is stronger than the homeotropic one), as before we assume $\bar{\theta}_1 = \pi/2$, $\bar{\theta}_2 = 0$ and the system of coordinates is chosen so that $\bar{\varphi}_1 \equiv 0$.

The conventional uniform planar and HAN ground states (see Fig. 1 a) b)) can be found for a vanishingly small azimuthal anchoring $L_{\varphi_i} \gg L_{\theta_i}$ and $\bar{\varphi}_2 = 0, \pi/2$. Interestingly, if $\bar{\varphi}_2 \in (0, \pi/2)$ is an arbitrary angle, the boundary conditions (10) are satisfied if and only if $\varphi_1 \neq \varphi_2$ or $\theta_1 = \theta_2 = 0$, irrespective of the smallness of the anchoring strength W_{φ_i} . The planar state becomes linearly unstable with respect to the twisted state if $L_{\varphi_2} - L_{\varphi_1} < h < L_{\theta_2} - L_{\theta_1}$. The states a) and c) become unstable with respect to the small perturbations of the polar angle θ , resulting in states b) and d), respectively, if the thickness

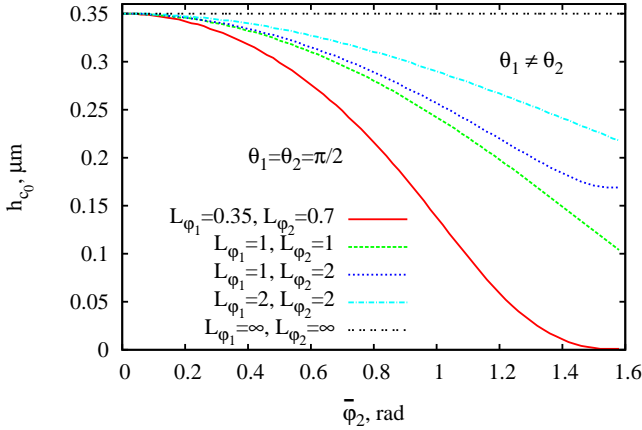


Fig. 2. The critical thickness (11) between planar (or twisted) states with $\theta_1 = \theta_2 = \pi/2$ and HAN (or twist-bend) states with $\theta_1 \neq \theta_2$. As before we fix $L_{\varphi_1} = 0.35 \mu\text{m}$ and $L_{\varphi_2} = 0.7 \mu\text{m}$, yielding $h_{c_0} = 0.35 \mu\text{m}$ for $\bar{\varphi}_2 = 0$ or $L_{\varphi_i} \rightarrow \infty$.

of the nematic film satisfies the following inequality

$$h(L_{\varphi_1} - L_{\theta_1} \sin^2 \varphi_1)(L_{\varphi_2} + L_{\theta_2} \sin^2(\varphi_2 - \bar{\varphi}_2)) > L_{\varphi_1} L_{\varphi_2} \times (L_{\theta_2} - L_{\theta_1}) - L_{\theta_1} L_{\theta_2} (L_{\varphi_2} \sin^2 \varphi_1 + L_{\varphi_1} \sin^2(\varphi_2 - \bar{\varphi}_2)). \quad (11)$$

In the limit of the vanishing azimuthal anchoring (11) yields the known result for the critical thickness $h_{c_0} \equiv L_{\theta_2} - L_{\theta_1}$ (Barbero–Barberi [21]) between the planar and the HAN states. In presence of azimuthal anchoring the threshold h_{c_0} cannot be defined explicitly, because of the dependence of φ_1 and φ_2 on h through the boundary conditions (10). In Fig. 2 we plot the computed threshold h_{c_0} , which has a smaller value than the Barbero–Barberi result, meaning that in presence of azimuthal anchoring the homogeneous planar (or twisted) states are easily replaced by the HAN (or twist-bend). This non-trivial coupling of twist and bend modes in base states is the consequence of the coupled equations (8) and the projection of the director \mathbf{n} on the xy plane in (6).

In the following we study the relative stability of these base states with respect to the periodically distorted stripe state and quantify the role of the saddle-splay elastic constant. The latter favours the periodic distortions in x or y -directions versus the effect of azimuthal anchoring, suppressing the in-plane director distortions and thus the formation of stripes. The conventionally assumed degenerate azimuthal anchoring on liquid substrates, does not necessarily mean that LC molecules can align along any direction simultaneously without some energy cost. Rather it means that because of some microscopic (e.g. adsorption layer) or geometric [13] reasons there is a tendency of molecules to align (spontaneously or not) along a common preferred direction on substrate interface.

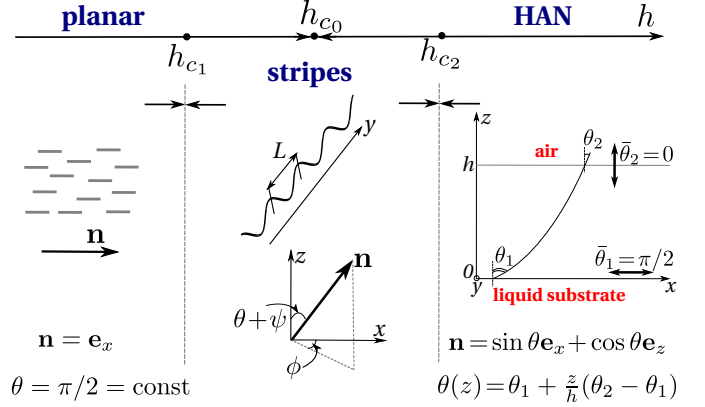


Fig. 3. Schematic representation of the structural phase transitions between the planar state, striped state ($h_{c_1} < h < h_{c_2}$) with periodicity L in the y -direction, and the hybrid aligned nematic, where the film thickness h is thought of as an order parameter. The critical thickness between the planar and HAN state is $h_{c_0} = L_{\theta_2} - L_{\theta_1}$ [21].

4 Linear stability analysis

In this section we assume the vanishing anchoring at the nematic–air interface $W_{\varphi_2} = 0$, yielding base states with $\varphi = 0$, so that we are dealing with the homogeneous planar state $\theta = \pi/2$ ($h < h_{c_0}$) or with the HAN state $\theta(\tilde{z}) = \theta_1 + (\theta_2 - \theta_1)\tilde{z}$ ($h > h_{c_0}$) as shown schematically in Fig. 3. To find the critical thresholds for the formation of stripes we consider the variation of the total free energy $\mathcal{F} = \mathcal{F}_b + \mathcal{F}_s + \mathcal{F}_a$ given by the equations (4)–(6) with respect to the small perturbation of the director \mathbf{n} (3). The perturbation angles ψ (polar) and ϕ (azimuthal) are assumed to be small $O(\varepsilon)$ with periodic modulation in y -direction

$$\psi(\tilde{y}, \tilde{z}) = \varepsilon f(\tilde{z}) \sin(\chi \tilde{y}), \quad \phi(\tilde{y}, \tilde{z}) = \varepsilon g(\tilde{z}) \cos(\chi \tilde{y}), \quad (12)$$

where $\tilde{y} = y/h$ is the dimensionless coordinate, and $\chi = 2\pi h/L$ is the wavenumber, with L being the period of stripes. Close to the instability threshold we can introduce a small parameter ε , defined as $h = h_c(1 + \varepsilon^2)$, where h_c is the critical thickness, characterising the instability of planar (HAN) states towards the stripe state. The difference in the total free energy of the stripe state and the base state can be written as the Taylor series $\delta\mathcal{F} = \varepsilon^2 \delta\mathcal{F}^{(2)} + \varepsilon^4 \delta\mathcal{F}^{(4)} + \dots$, with

$$\delta\mathcal{F}^{(2)} = \frac{K\chi}{4\pi h} \int_0^{2\pi} d\tilde{y} \left[\int_0^1 d\tilde{z} \left\{ \sin^2 \theta(\tilde{z}) [(\partial_{\tilde{z}} \phi)^2 + (\partial_{\tilde{y}} \phi)^2] + (\partial_{\tilde{z}} \psi)^2 + (\partial_{\tilde{y}} \psi)^2 \right\} + \frac{h \sin^2 \theta_1}{L_{\varphi_1}} \phi(0)^2 - \frac{h \cos 2\theta_1}{L_{\theta_1}} \psi(0)^2 + \frac{h \cos 2\theta_2}{L_{\theta_2}} \psi(1)^2 + 2\nu \sin^2 \theta \psi \partial_{\tilde{y}} \phi \Big|_{\tilde{z}=0}^{\tilde{z}=1} \right], \quad (13)$$

where $\nu = K_{24}/K$ is another dimensionless parameter. The value of K_{24} as well as the extrapolation length for azimuthal anchoring L_{φ_1} are not precisely known, therefore we present below our results for the critical threshold as function of ν and L_{φ_1} .

The Euler–Lagrange equations associated with (13) are

$$\partial_{\tilde{z}} \tilde{z} f - \chi^2 f = 0, \quad (14a)$$

$$\partial_{\tilde{z}} (\sin^2 \theta \partial_{\tilde{z}} g) - \chi^2 \sin^2 \theta g = 0, \quad (14b)$$

with the general solution given by:

$$f(\tilde{z}) = C_1 e^{\chi \tilde{z}} + C_2 e^{-\chi \tilde{z}}, \quad (15a)$$

$$g(\tilde{z}) = \frac{C_3 e^{\lambda \tilde{z}} + C_4 e^{-\lambda \tilde{z}}}{\sin \theta(\tilde{z})}, \quad (15b)$$

where $\theta(\tilde{z}) = \theta_1 + (\theta_2 - \theta_1)\tilde{z}$ and $\lambda = \sqrt{\chi^2 - (\theta_2 - \theta_1)^2}$. In the planar case $\theta = \pi/2$ equation (15)b simplifies to the sum of two exponents. The integration constants C_i can be found from the boundary conditions, written in the matrix form as $\sum_{i=1}^4 \mathcal{M}_{ij} C_i = 0$, where

$$\mathcal{M} = \begin{pmatrix} -\chi - \frac{h \cos 2\theta_1}{L_{\theta_1}} & \chi - \frac{h \cos 2\theta_1}{L_{\theta_1}} & \nu \chi \sin \theta_1 & \nu \chi \sin \theta_1 \\ \frac{e^{\chi(L_{\theta_2}\chi + h \cos 2\theta_2)}}{L_{\theta_2}} & \frac{e^{-\chi(h \cos 2\theta_2 - L_{\theta_2}\chi)}}{L_{\theta_2}} & -\nu e^{\lambda} \chi \sin \theta_2 & -\nu e^{-\lambda} \chi \sin \theta_2 \\ \nu \chi & \nu \chi & \frac{h - L_{\varphi_1} \lambda + L_{\varphi_1}(\theta_2 - \theta_1) \cot \theta_1}{\sin \theta_1 L_{\varphi_1}} & \frac{h + L_{\varphi_1} \lambda + L_{\varphi_1}(\theta_2 - \theta_1) \cot \theta_1}{\sin \theta_1 L_{\varphi_1}} \\ -\nu \chi e^{\chi} & -\nu \chi e^{-\chi} & \frac{e^{\lambda}(\lambda - (\theta_2 - \theta_1) \cot \theta_2)}{\sin \theta_2} & -\frac{e^{-\lambda}(\lambda + (\theta_2 - \theta_1) \cot \theta_2)}{\sin \theta_2} \end{pmatrix}. \quad (16)$$

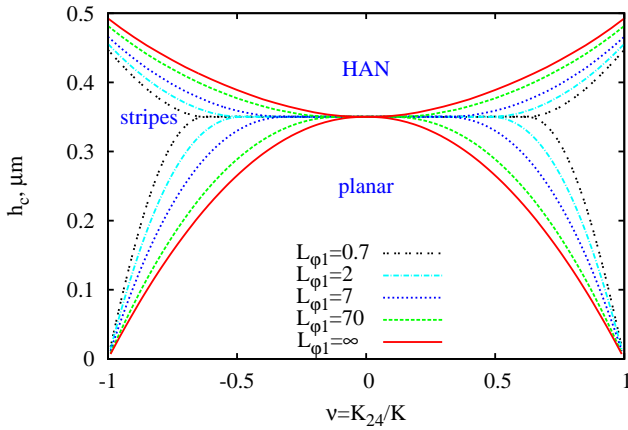


Fig. 4. The critical thickness, characterising the lower (h_{c_1}) and the upper (h_{c_2}) instability thresholds as function of saddle–splay elastic constant $\nu = K_{24}/K$. The stripe phase exists between the curves of the same colour and it is restrained when L_{φ_1} decreases or azimuthal anchoring at nematic–liquid substrate interface W_{φ_1} increases. The values for the polar anchoring are known $L_{\theta_1} = 0.35 \mu\text{m}$ and $L_{\theta_2} = 0.7 \mu\text{m}$ [7,15].

The nontrivial solution ($C_i \neq 0$) exists if and only if the determinant of the matrix (16) is zero, $\det \mathcal{M} = 0$. This condition gives the relationship between the thickness h of the nematic film, the dimensionless wavenumber χ , the angles $\theta_{1,2}$ (HAN case) and other parameters of the system. Since the critical thickness of the nematic film h_c is unknown, the problem should be solved consistently together with the boundary conditions for the equilibrium angles θ_i (10)a-b, which in turn also depend on h . The minimum of the curves $\det \mathcal{M} = 0$ in the h – χ plane allows to identify the critical thickness h_c and the critical wavenumber χ_c at the bifurcation point, for a given value of ν , and the extrapolation length of azimuthal anchoring

L_{φ_1} , while the polar anchoring is known $L_{\theta_1} = 0.35 \mu\text{m}$, $L_{\theta_2} = 0.7 \mu\text{m}$ [7,15]. In Fig. 4 we plot h_c , characterising the planar–stripe (h_{c_1}) and the HAN–stripe (h_{c_2}) instability thresholds. The curves are symmetric around $\nu = 0$. In presence of strong azimuthal anchoring (small values of L_{φ_1}) the formation of a stripe phase is suppressed, as was predicted in [22]. Experimentally compatible values for critical thickness $h_{c_1} \simeq 40 \text{ nm}$ and $h_{c_2} \simeq 0.5 \mu\text{m}$ occur at $|\nu| \simeq 1$ and for L_{φ_1} of order of tens of micron, corresponding to extremely weak azimuthal anchoring. Indeed, according to [16] the value of the azimuthal anchoring should be one or two orders of magnitude smaller than the polar anchoring, which is confirmed by experiments [23] for example, where extrapolation lengths L_{φ_i} up to $80 \mu\text{m}$ were measured. Other experiments using the dynamic light scattering [24], on the contrary, suggest that the polar and the azimuthal anchoring are of the same order of magnitude.

In Fig. 5 we plot the critical wavenumber χ_{c_i} at h_{c_i} , with one inverse branch for illustrative purposes. As mentioned above, the experimentally relevant critical thickness h_{c_i} occurs at $K_{24} \simeq K$ and $L_{\varphi_1} \simeq 70 \mu\text{m}$, yielding the critical wavenumbers $\chi_{c_1} \simeq 0.2$ and $\chi_{c_2} \simeq 0.1$. For planar–stripe instability χ vanishes only in the limit of $L_{\varphi_1} \rightarrow \infty$ ($W_{\varphi_1} = 0$), while for HAN–stripe instability $\chi = 0$ is always the solution of $\det \mathcal{M} = 0$. Comparing the results on h_{c_1} and χ_{c_1} with our previous analysis [10], where we have taken into account the twist elastic constant $K_{22} \neq K_{11}$ and assumed a non-zero azimuthal anchoring at nematic–air interface, we conclude that the predictions of both critical parameters agree quantitatively. This plausibly means that the ratio K_{22}/K_{11} does not play a dominant role in our system and that the one constant approximation is reasonable to analyse the stripe instability. It is hard to directly compare theoretical predictions of the upper threshold h_{c_2} and χ_{c_2} with experimental data, because of the presence of defects in nematic films thicker than $h \simeq 0.5 \mu\text{m}$ [5,8,9]. The HAN state, therefore, is an idealised director’s configuration which is probably not ac-

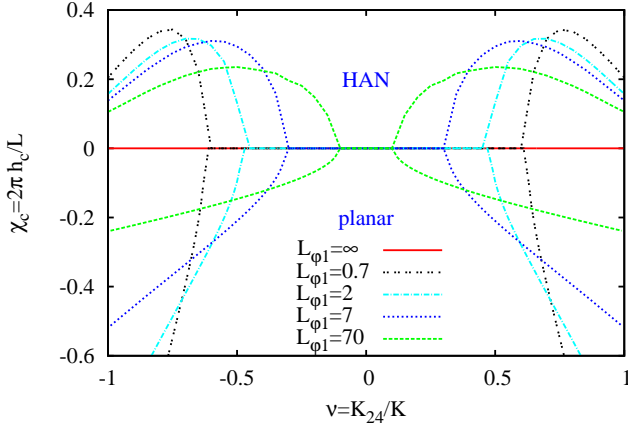


Fig. 5. The critical wavenumber χ_{c1} and χ_{c2} , characterising the lower and the upper instability thresholds, respectively. In the limit of the vanishing azimuthal anchoring $L_{\varphi_1} \rightarrow \infty$ the wavelength of stripes vanishes.

cessible in real systems, because of the presence of defects. For completeness in Fig. 6 we plot the equilibrium angles $\theta_{1,2}$ found at h_{c2} and satisfying the boundary conditions (10)a-b.

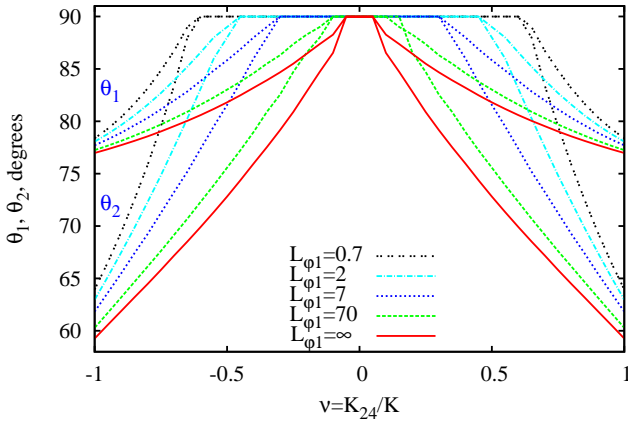


Fig. 6. The equilibrium angles $\theta_{1,2}$, satisfying the boundary conditions (10)a,b (for $\varphi = 0$) at the critical thickness h_{c2} (see Fig. 4). The values for the polar anchoring are known $L_{\theta_1} = 0.35 \mu\text{m}$ and $L_{\theta_2} = 0.7 \mu\text{m}$ [7,15].

5 Perturbation of the twisted state

It was realised by Lavrentovich [13] that, unlike flat parallel interfaces, the tilt of interfaces with respect to each other (wedge geometry) results in breaking the azimuthal degeneracy. This simple geometrical argument was used later to analyse the wetting behaviour of 5CB on glycerol [4], where the profile of the spreading nematic drop

varies with distance from the centre of the drop, resulting in gradients of the thickness. Thickness gradients of spreading drops are easily obtained on glycerol rather than on water [6,9], suggesting an azimuthal anchoring being stronger on water. One can imagine that, similar to the wedge geometry, locally spreading drops have also two preferred directions for alignment i) along the gradient of the thickness and ii) in mutually orthogonal in the tangential plane to the nematic–air interface. Then the preferred alignment of director is parallel to one of the wedge sides, namely $\bar{\varphi}_2 = 0, \pi/2$ in our system of coordinates. The generally assumed case $\bar{\varphi}_2 = 0$, when the free energy of nematic LC constrained between two isotropic substrates does not depend on φ [2], was considered in the previous section. We will focus below on the case with $\bar{\varphi}_2 = \pi/2$, resulting in a tendency of the director to form a twist configuration with $\varphi_1 \neq \varphi_2$. There might be other possibilities for breaking the in-plane degeneracy, e.g. magnetic fields, which would result in W_{φ_i} , dependent on a particular experiment, contrary to the polar anchoring being an intrinsic parameter of the system.

In this section we perform the linear stability analysis, starting from the ground state with azimuthal angle $\varphi(\tilde{z})$ varying along the thickness of the film. The small undulations of the director \mathbf{n} (3) is written in terms of periodic distortions of the polar θ and the azimuthal φ angles, respectively,

$$\psi(\tilde{x}, \tilde{y}, \tilde{z}) = \varepsilon f(\tilde{z}) e^{i\chi_x \tilde{x} + i\chi_y \tilde{y}}, \quad \phi(\tilde{x}, \tilde{y}, \tilde{z}) = \varepsilon g(\tilde{z}) e^{i\chi_x \tilde{x} + i\chi_y \tilde{y}}, \quad (17)$$

where the dimensionless wavenumbers $\chi_x = 2\pi h/L_x$ and $\chi_y = 2\pi h/L_y$ are related to the periodicity of stripes L_x and L_y , in x and y directions, respectively, $\tilde{x} = x/h$ and $\varepsilon < 1$. The functions $f(\tilde{z})$ and $g(\tilde{z})$ in (17) should satisfy the system of linearised equilibrium equations given by (for details see the appendix, in particular (21))

$$\partial_{\tilde{z}\tilde{z}} f - (\chi^2 + \cos 2\theta (\partial_{\tilde{z}} \varphi)^2) f - \sin 2\theta \partial_{\tilde{z}} \varphi \partial_{\tilde{z}} g = 0, \quad (18a)$$

$$\partial_{\tilde{z}} (\sin^2 \theta \partial_{\tilde{z}} g) - \chi^2 \sin^2 \theta g + \sin 2\theta \partial_{\tilde{z}} \varphi f = 0, \quad (18b)$$

where $\chi^2 = \chi_x^2 + \chi_y^2$, θ and φ are defined by (9). Although this system is linear we will focus below only on the twisted state with $\theta \equiv \pi/2$, when the perturbed solution can be written in the closed form as

$$f(\tilde{z}) = C_1 e^{\sqrt{\chi^2 - (\varphi_2 - \varphi_1)^2} \tilde{z}} + C_2 e^{-\sqrt{\chi^2 - (\varphi_2 - \varphi_1)^2} \tilde{z}}, \quad (19a)$$

$$g(\tilde{z}) = C_3 e^{\chi \tilde{z}} + C_4 e^{-\chi \tilde{z}}. \quad (19b)$$

Similar to the analysis in section 4 we can write the related boundary conditions (see appendix (24)) in the matrix form as $\sum_{i=1}^4 \mathcal{M}_{ij} C_i = 0$. If the determinant of the matrix is positive, $\det \mathcal{M} > 0$ the twisted state with $C_i = 0$ is stable, otherwise an instability towards a periodically distorted state occurs.

As an example, in Fig. 7 we plot the sign of $\det \mathcal{M}$ in h – χ plane, where we have assumed perturbations in either x or y -direction. The azimuthal anchoring is equal at both interfaces to guarantee the non-planar base state with $\varphi_1 \neq \varphi_2 \neq 0$. For the weak azimuthal anchoring

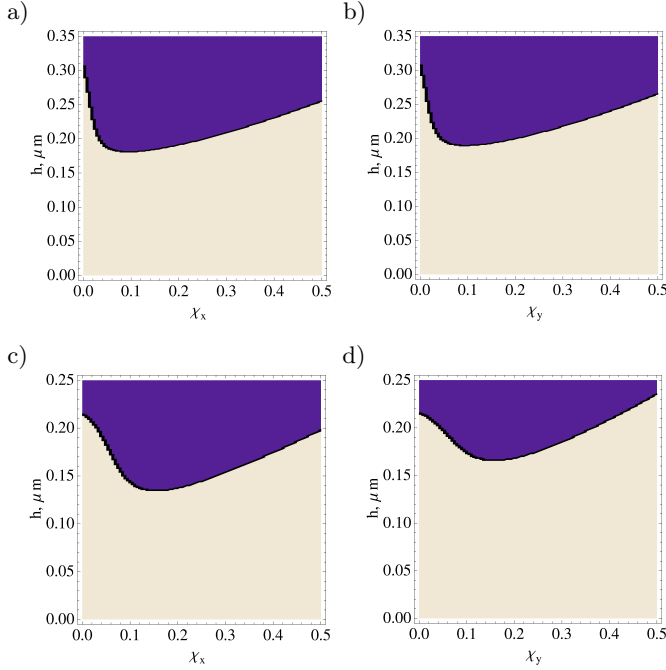


Fig. 7. The light (dark) regions correspond to the stable (unstable) twist state with $\theta = \pi/2$ and $\varphi = \varphi_1 + (\varphi_2 - \varphi_1)\tilde{z}$. The minimum of the curves separating two colours gives the lower threshold for the formation of stripes in either x -direction, χ_x (a, c) or in y -direction χ_y (b, d). The choice of parameters is $L_{\theta_1} = 0.35 \mu\text{m}$, $L_{\theta_2} = 0.7 \mu\text{m}$, $|\nu| = 0.95$, $L_{\varphi_1} = L_{\varphi_2} = 10 \mu\text{m}$ for (a, b) and $L_{\varphi_1} = L_{\varphi_2} = 2 \mu\text{m}$ for (c, d).

$L_{\varphi_1} = L_{\varphi_2} = 10 \mu\text{m}$ (Fig. 7a, b), falling into the range predicted by Sparavigna et al [3] for 5 CB on glycerol system, we find a similar threshold $h_c \approx 0.180 \mu\text{m}$ and $\chi_c \approx 0.1$ for stripes in both x and y direction. This result may be related to experimental observations of the squared pattern [5,7], which can be thought of as the superposition of stripes with similar wavelength running in mutually orthogonal directions. In the case of stronger azimuthal anchoring $L_{\varphi_1} = L_{\varphi_2} = 2 \mu\text{m}$ the threshold thickness decreases, which is more pronounced for stripes in x -direction $h_{c_x} \approx 0.13 \mu\text{m}$ compared to y -direction $h_{c_y} \approx 0.16 \mu\text{m}$ (Fig. 7c, d). This results is contrary to the case of the planar-stripe instability, when striped domains are suppressed in presence of azimuthal anchoring (see Fig. 4).

6 Weakly nonlinear analysis

The linear stability analysis, considered above allows to identify the critical thickness and the critical wavenumber at the instability threshold. However the linearised boundary conditions (16) give only the ratio of the integration constants C_i . Thus, the perturbation functions ϕ and ψ are *known* up to some multiplying factor A , called the amplitude of perturbation. To eliminate this uncertainty and to find A we expand the total free energy further in powers

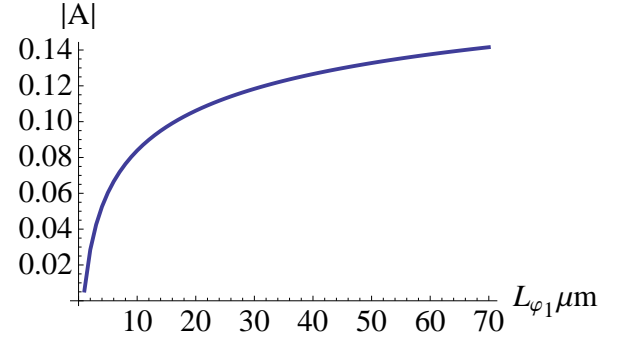


Fig. 8. The amplitude for the planar-stripe instability as function of the azimuthal anchoring L_{φ_1} . The choice of parameters is $L_{\theta_1} = 0.35 \mu\text{m}$, $L_{\theta_2} = 0.7 \mu\text{m}$, $|\nu| = 0.95$, $L_{\varphi_2} = 0$ and the corresponding thresholds are found in section 4.

of ε up to $O(\varepsilon^4)$, fourth order in ϕ and ψ . Moreover, we assume to be in the vicinity of the threshold h_c, χ_c , and the thickness of the film given by $h = h_c(1 + \varepsilon^2)$ is the control parameter of our system, with $\varepsilon \ll 1$ measuring the distance from the threshold. Then the Taylor expansion of the free energy is

$$\delta\mathcal{F} = \varepsilon^2 A^2 \delta\mathcal{F}^{(2)} + \varepsilon^4 (A^2 \delta\mathcal{F}_a^{(2)} + A^4 \delta\mathcal{F}^{(4)}) + O(\varepsilon^6), \quad (20)$$

where $\delta\mathcal{F}^{(2)}$ is given by (13) for planar (HAN) case, and as the sum of (21)–(23) for the twisted (twist-bend) case, $\delta\mathcal{F}_a^{(2)}$ is the second order contribution of the anchoring energy (23) and $\delta\mathcal{F}^{(4)}$ is the fourth order contribution of the total energy, expanded in ϕ and ψ . We make use of *Mathematica* to integrate directly (20), since the functions ϕ and ψ (15), (19) as well as the critical point were found before in sections 4, 5. The first term vanishes at the critical point $\delta\mathcal{F}^{(2)}|_{h=h_c, \chi=\chi_c} = 0$, as expected. Then the amplitude can be identified by extremising the next order term, namely $A^2 = -\delta\mathcal{F}_a^{(2)} / (2\delta\mathcal{F}^{(4)})|_{h=h_c, \chi=\chi_c}$. As pointed out in [25] this procedure may be equivalent to the derivation of the amplitude equations. The energy method, however, does not allow to find a nonlinear change in the wavelength.

In Fig. 8 we plot the amplitude A for the planar-stripe instability as function of the azimuthal anchoring L_{φ_1} . The increase of A with L_{φ_1} suggests the suppression of the stripe phase in presence of strong azimuthal anchoring, which also agrees with the linear stability analysis performed in section 4. For all considered values of L_{φ_1} the amplitude is $O(1)$, justifying the perturbation approach developed above.

7 Concluding remarks

We have reconsidered the stripe instability in thin nematic films, subjected to antagonistic boundary conditions. The thickness of the film as well as azimuthal anchoring were treated as extrinsic parameters of our system related to a particular experiment, while the polar anchoring and

the saddle-splay elasticity being intrinsic ones. Within the one constant approximation we have shown the possibility of different base states, admitting twist and bend of the nematic director. Solving the variational problem we identified the critical thickness and the critical wavenumber, which determine the threshold of stripe instability. Moreover, the perturbation of the twisted base state can account for the formation of the long-wavelength stripes in mutually orthogonal directions, observed in recent experiments [5,7]. Considering different base states can be useful for comparing theoretical predictions with experimental observations, in particular for thin nematic films with not well defined base state. In future it can be also important to account for thickness gradients of nematic films which was left outside the scope of this paper.

It is our pleasure to acknowledge the stimulating discussions with Anne-Marie Cazabat. O.V.M. was partly supported by the French National Research Agency (ANR), grant ANR-07-BLAN-0158.

A The variation of the free energy

In this appendix we aim to find the variation of the free energy with respect to the perturbation of the director \mathbf{n} (3), such that $\theta \rightarrow \theta + \psi$ and $\varphi \rightarrow \varphi + \phi$. The angles $\theta(\tilde{z})$, $\varphi(\tilde{z})$ describe the base state of the nematic discussed in section 3 and the angles $\psi(\tilde{x}, \tilde{y}, \tilde{z})$, $\phi(\tilde{x}, \tilde{y}, \tilde{z})$ are $O(\varepsilon)$. The case $\varphi(\tilde{z}) \equiv 0$ was considered in section 4, yielding the free energy variation $\delta\mathcal{F}^{(2)}$ (13) in the harmonic approximation. Assuming a general case with θ and φ both changing along the thickness of the film and expanding the free energy density up to ε^2 we find the bulk contribution associated with (4) as

$$f_b^{(2)} = |\nabla\psi|^2 + \sin^2\theta |\nabla\phi|^2 + \cos(2\theta)\varphi_{,\tilde{z}}^2\psi^2 + 2\sin(2\theta)\varphi_{,\tilde{z}}\psi\phi_{,\tilde{z}}, \quad (21)$$

where the subscript $_{,\tilde{z}}$ stands for the derivative with respect to \tilde{z} . Taking into account that ϕ and ψ are periodic functions $\partial_x\phi^2 = 0$, $\partial_y\phi^2 = 0$ and $\partial_x(\phi\psi) = 0$, $\partial_y(\phi\psi) = 0$, the perturbation of the saddle-splay term (5) results in

$$f_s^{(2)} = 2\nu \sin^2\theta \left[\sin\varphi \phi\psi_{,\tilde{x}} - \cos\varphi \phi\psi_{,\tilde{y}} \right] \Big|_{\tilde{z}=0}^{\tilde{z}=1}. \quad (22)$$

Finally the variation of the anchoring contribution (6) takes the form

$$f_a^{(2)} = \sum_{i=1,2} \left(\frac{h \cos 2(\theta_i - \bar{\theta}_i) \psi^2}{L_{\theta_i}} + \frac{h \cos 2\theta_i \sin^2(\varphi_i - \bar{\varphi}_i) \psi^2}{L_{\varphi_i}} + \frac{h \sin^2\theta_i \cos 2(\varphi_i - \bar{\varphi}_i) \phi^2}{L_{\varphi_i}} \right) \Big|_{\tilde{z}=\tilde{z}_i}, \quad (23)$$

where the index $i = 1$ stands for the nematic-substrate interface ($\tilde{z}_1 = 0$) characterised by $\bar{\theta}_1 = \pi/2$ and $\bar{\varphi}_1 = 0$, the index $i = 2$ ($\tilde{z}_2 = 1$) is related to nematic-air interface with $\bar{\theta}_2 = 0$ and $\bar{\varphi}_2 = \pi/2$. The boundary conditions associated

with (21)–(23) can be expressed as

$$\left(\frac{\partial f_b^{(2)}}{\partial \psi_{,\tilde{z}}} + \frac{d}{d\tilde{x}} \frac{\partial f_s^{(2)}}{\partial \psi_{,\tilde{x}}} + \frac{d}{d\tilde{y}} \frac{\partial f_s^{(2)}}{\partial \psi_{,\tilde{y}}} - \frac{\partial f_a^{(2)}}{\partial \psi} \right) \Big|_{\tilde{z}=0} = 0, \quad (24a)$$

$$\left(\frac{\partial f_b^{(2)}}{\partial \psi_{,\tilde{z}}} - \frac{d}{d\tilde{x}} \frac{\partial f_s^{(2)}}{\partial \psi_{,\tilde{x}}} - \frac{d}{d\tilde{y}} \frac{\partial f_s^{(2)}}{\partial \psi_{,\tilde{y}}} + \frac{\partial f_a^{(2)}}{\partial \psi} \right) \Big|_{\tilde{z}=1} = 0, \quad (24b)$$

$$\left(\frac{\partial f_b^{(2)}}{\partial \phi_{,\tilde{z}}} - \frac{\partial(f_s^{(2)} + f_a^{(2)})}{\partial \phi} \right) \Big|_{\tilde{z}=0} = 0, \quad (24c)$$

$$\left(\frac{\partial f_b^{(2)}}{\partial \phi_{,\tilde{z}}} + \frac{\partial(f_s^{(2)} + f_a^{(2)})}{\partial \phi} \right) \Big|_{\tilde{z}=1} = 0. \quad (24d)$$

References

1. Lavrentovich, O. D. and Pergamenschchik, V. M. (1994) *Phys. Rev. Lett.* **73**, 979.
2. Lavrentovich, O. D. and Pergamenschchik, V. M. (1995) *Int. J. Mod. Phys. B* **9**, 2389.
3. Sparavigna, A., Komitov, L., Lavrentovich, O. D., and Strigazzi, A. (1992) *J. Phys. II France* **2**, 1881.
4. Sparavigna, A., Lavrentovich, O. D., and Strigazzi, A. (1994) *Phys. Rev. E* **249**, 1344.
5. Delabre, U., Richard, C., Guèna, G., Meunier, J., and Cazabat, A.-M. (2008) *Langmuir* **24**, 3998.
6. Delabre, U., Richard, C., and Cazabat, A. M. (2009) *J. Phys.: Condens. Matter* **21**, 464129.
7. Delabre, U., Richard, C., and Cazabat, A. M. (2009) *J. Phys. Chem. B* **113**, 3647.
8. Delabre, U., Richard, C., Yip Cheung Sang, Y., and Cazabat, A. M. (2011) *Langmuir* **26**, 13368.
9. Cazabat, A. M., Delabre, U., Richard, C., and Yip Cheung Sang, Y. (2011) *Adv. Colloid Interface Sci.* **168**, 29.
10. Manyuhina, O. V., Cazabat, A. M., and Ben Amar, M. (2010) *EPL* **92**, 16005.
11. Alexe-Ionescu, A. L., Barbero, G., and Lelidis, I. (2002) *Phys. Rev. E* **66**, 061705.
12. Barbero, G., Lelidis, I., and Zvezdin, A. K. (2003) *Phys. Rev. E* **67**, 051708.
13. Lavrentovich, O. D. (1992) *Phys. Rev. A* **46**, R722.
14. Sparavigna, A., Lavrentovich, O. D., and Strigazzi, A. (1995) *Phys. Rev. E* **51**, 792.
15. Delabre, U. Films nématiques minces sur substrats liquides PhD thesis University Pierre et Marie Curie Paris (2009).
16. Jerome, B. (1991) *Rep. Prog. Phys.* **54**, 391.
17. deGennes, P. G. and Prost, J. (1993) *The Physics of Liquid Crystals*, Clarendon, Oxford.
18. The following identity $(\nabla \cdot \mathbf{n})^2 + (\mathbf{n} \cdot \nabla \times \mathbf{n})^2 + |\mathbf{n} \times \nabla \times \mathbf{n}|^2 \equiv |\nabla \mathbf{n}|^2 + \nabla \cdot [(\nabla \cdot \mathbf{n})\mathbf{n} + \mathbf{n} \times \nabla \times \mathbf{n}]$ allows to transform the Frank energy with equal contributions from splay, twist and bend terms on the left-hand side, respectively, to equation (1).
19. Ericksen, J. L. (1966) *Phys. Fluids* **9**, 1205.
20. Faetti, S. (1990) *Mol. Cryst. Liq. Cryst* **179**, 217.
21. Barbero, G. and Barberi, R. (1983) *J. Physique* **44**, 609.
22. Sparavigna, A., Komitov, L., Stebler, B., and Strigazzi, A. (1991) *Mol. Cryst. Liq. Cryst.* **207**, 265.
23. Nespoulous, M., Blanc, C., and Nobili, M. (2007) *J. Appl. Phys.* **102**, 073519.
24. Vilfan, M., Mertelj, A., and Copic, M. (2002) *Phys. Rev. E* **65**, 041712.
25. Napoli, G. and Turzi, S. (2008) *Comput. Math. Appl* **55**, 299.